Research paper

Investigation of process parameters for T-joint aluminum alloy 6061-T6 with nanocomposites material friction stir welding based on the Taguchi method

Faiz F. Mustafa[*] **and Sadoon R. Daham**

Department of Automated Manufacturing Engineering, Al-Khwarizmi College of Engineering, University of Baghdad, Baghdad,10070, Iraq

Article info:	

Abstract

Surface layer in many engineering applications is strengthened by ceramic grains where the main parts have higher structure toughness than the original material. This paper presents the effect of four process parameters that have been taken into consideration using Taguchi technique based on L9 orthogonal array. These parameters are;1) transverse speed, 2) type of nano- powders, 3) rotational speed, and 4) groove's depth friction stir welding T-joints aluminum alloy 6061-T6. This work combines welding T-joint sections and creating MMNCs in welding region simultaneously. The predicted optimum parameters and their percentage of contribution are estimated, utilizing the analysis of variance and signal to noise ratio techniques, depending on tensile test in skin and stringers direction, and hardness test of the joint. Optical microscope and scanning electron microscope (SEM) analysis are used to verify the microstructure and dispersion of nano-powders in welding joint. The best ultimate tensile stress (UTSskin) equal to (177MPa) for the skin welded part was obtained at the optimal conditions of 1550rpm rotational speed, 15mm/min transverse speed, Al_2O_3 type of powder and 1mm groove's depth. SEM micrographic for metal matrix nanocomposite of all nine experiments revealed that the nano-particles are irregularly dispersed in nugget zone due to one pass. The rotational speeds of 960rpm, the transverse speed of 15mm/min, type of powder TiO_2, and groove's depth of 1.5mm, give the greatest hardness value of 80HV in nugget zone. The analysis of variance shows that the groove's depth is the most significant parameter in this investigation.

1. Introduction

As a new solid-state joining technique, the friction stir welding (FSW) has been developed for more than two decades This technique has been developed in The Welding Institute (UK), for welding aluminum alloys that were difficult to weld by using traditional welding techniques

101

[1]. Due to its high strength, light weight and high corrosion resistance, aluminum alloy 6061-T6 is commonly used in aerospace, defense, vehicles and marine areas. But, it exhibits inferior tribological properties in extensive usage [2-4]. Thus, aluminum-based metal matrix composites, strengthened with ceramics particles production, are created as another alrenative to materials with better quality, a good weight proportion and quality to cost proportion, high firmness, and great solidness, which impact on enhancing wear resistance, hardness and erosion resistance [5-8]. Therefore, implementing a suitable method for refining the microstructure and homogeneous dissipation of reinforcements on alloy surface will improve the sliding wear actions for welding joints [9]. A lot of challenges exist with the conventional surface modification techniques either during the desperation of the reinforcement particles on the metal surface or with the control of their dispersal [10].

T-joints are an important welding technique in which the rigidity and strength of the skin can be improved and strengthened by stringers without a significant increase in weight [11]. A special design represented by revolving pins into clamped blanks has been introduced to the FSW of the T-joints as appeared in Fig. 1. The special design has been constructed by inserting the pins with a tilt angle, which was employed to set the contact between the tool shoulder and the blank. As the pin is inserted into the upper sheet (skin), the blank material undergoes a local back-and-forward extrusion process to penetrate the vertical blank (stringer), while the tool shoulders touched the upper sheet. Then, the friction forces and material deformation are considered the main reason for increasing the temperature of the material due to rotational tool. The two blank materials are softened as the tool is moved along the joint (without melting) and mixed to perform the weld joint [12].

Tavares et al [13] studied the effects of process parameters such as transverse speed, vertical downward force, and rotational speed on both T-joint and butt joint. Two types of Al alloys were used in their work. The skin plate is made of Al 6056-T4, and the stringers plate is made of Al 7000 series. Bending test, the fatigue test, and microhardness were done for all experiments. Lima et al [14] studied the influence of processing parameters on particle dispersal.
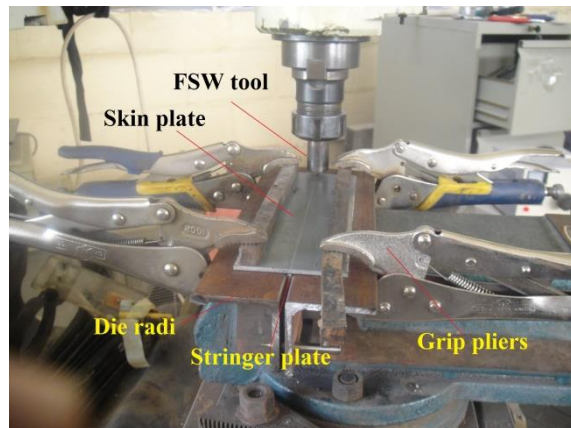
Fig. 1. T-joints clamping fixture for FSW process.

Hardness was tested in Al-alloy and improved by friction stir processing (FSP) with multi-walled carbon nanotubes. TEM and SEM show that nanotubes are etched in the lamellae zones of the Al-alloy stir region and that they are preserved in multi-walled.

Shafiei-Zarghani et al [15] utilized a new technique of using the FSP to induce the nano-sized Al_2O_3 into 6082 Al alloys to create a composite surface layer. Samples were used in multiple numbers of FSP passes from one to four, with and without Al_2O_3 powder. Azizieh et al [16] studied the effects of rotational speed, pin profile and the number of FSP passes on the distribution of nano-powders and matrix microstructure. The grain refinement of the matrix and enhanced distribution of nano-powders were achieved after each FSP pass. Friction stir process was utilized to produce $AZ31/Al_2O_3$ nanocomposites for surface applications. Mahmoud et al [17] studied the effects of reinforced composites with mixtures of SiC and Al2O3 particles of an average size of 1,25μm produced on the 5 mm thick aluminum plate A 1050-H24 by friction stir processing FSP; and their wear resistance as a function of the relative weight ratios of the particles. Salehi et al [18] used the design of the experiment (DOE) to decide the most significant determinant which affects ultimate tensile strength (UTS) of AA6061/SiC nanocomposites created by FSP. The influence of four determinants, including transverse speed, rotational speed, pin profile, and tool penetration depth on the ultimate tensile stress was examined by Taguchi method to specify the best process parameters. Zhenglin et

al. [19] studied FSP on AA6061-T6 with and without additions of multi-walled CNTs. For FSP on monolithic Al plates, dendrites were broken down and distributed equally by increasing the number of the passes. The hardness and tensile yield strength of the FSP improved with the addition of CNT compared to the FSP of AA6061-T6 without CNT. Takhakh and Abdulla [20] investigated the micorhardness of fabricated composite surface based on AA 7075-T651 matrix reinforced with micro-sized particles SiC by FSP. New tools with a hollow reservoir for ceramic powder having two holes in shoulder face were used to insert the ceramic powder from the cavity to processing zone with special mechanical system.

This study presents the effect of transvers speed, rotational speed, types of nano-powder, and groove's depth on the mechanical properties which are hardness, and microstructure of the nugget zone.

2. Experimental procedure

The chemical composition of AA 6061-T6 used in this study is represented in Table 1. The plates were machined into $(200 \times 70 \times 3)$ mm^3 for the skins and $(200 \times 30 \times 3)$ mm^3 for the stringers, as shown in Fig. 2. A groove was fabricated along and on the center of the skin plates with a width of 1.6 mm and variables depth of 0.5, 1, and 1.5 mm. The tool was machined out of HSS (AISI M2). They consisted of a shoulder with a diameter of 20 mm, and columnar probe with a diameter of 2.5 mm and length of 4.2 mm. Three types and attributes of commercially available nanoparticles were used and the details of these powders are given in Table 2. To prevent the nanoparticles from scattering out the groove during the FSW, the groove was covered firstly with a modified FSP tool that only had the same shoulder diameter without any probe. To fix the stringer under the skin, the researcher developed a fixture using the conventional "Turret Milling Machine Model: MDM 4VS/4HS/4 S" for performing FSW operation. The tensile test is performed on a servo-operated universal hydraulic test system at a load rate of 1.5 KN / min at a crosshead speed of 1 mm / min to undergo the deformation until the failure occurs. Fig. 3 shows the hoop and T-pull tensile stress test used to evaluate the ultimate tensile strength across skin and stringer of welded part.

The microstructure of the surface welded T-joints were examined and observed carefully to be normal to the FSW, mechanically polished with diamond metallographic polishing oil, and etched with Keller reagent (5% HNO$_3$, 3% HCL, 2% HF, and 190% H$_2$O for each 200 ml) for about 45 sec, by (Nikon TECHNO) optical microscopic (OM), and (TESCAN) Scanning Electron Microscopy (SEM).

The micro-hardness values were measured by a micro-Vickers hardness tester using a load of 200g for 10 sec. The hardness distribution was measured along two perpendicular lines through the mid-plane of the polished cross-sections of the nugget zone (NZ) with a separated distance of 0.25mm.

Table 1. Chemical composition of aluminum 6061-T6 alloy (wt. %).

Elements	Mg	Si	Cu	Zn	Ti	Mn	Cr	Al
Acq.	0.94	0.69	0.33	0.1	0.01	0.07	0.2	Balance

Table 2. Details of nano-powders.

Types of powder	Attributes
Aluminum Oxide (Al$_2$O$_3$)	Alpha, high purity 99.9% size 135 nm
Titanium Oxide (TiO$_2$)	Rutile, 96%, coated with silicon size 30 nm
Silicon Carbide (SiC)	Beta, 99%, cubic Size <80 nm
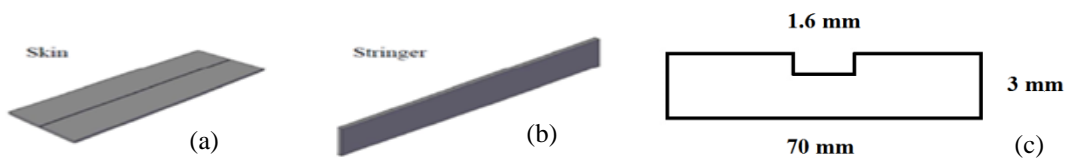
Fig. 2. Aluminum plat; (a) skin plate, (b) stringer plate and (c) groove in the centre of the skin.
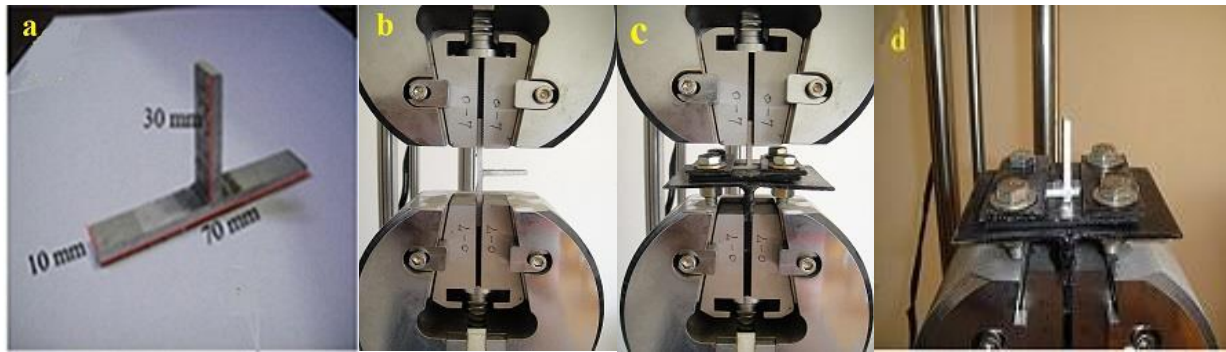
Fig. 3. Tensile test; (a) specimen tensile test, (b) hoop test, (c) T-pull test and (d) clamping.

Table 3. The parameters of FSW and their levels.

No.	Parameters		Code	Level1	Level2	Level3
1	Rotational Speed	rpm	A	960	1550	2000
2	Transverse Speed	mm/min	B	6	11	15
3	Type of powders	---------	C	Al_2O_3	SiC	TiO_2
4	Groove's depth	mm	D	0.5	1	1.5

3. Design of the experiment based on Taguchi's methods

3.1. The FSW parameter selection

In this study, in order to investigate the effect of FSW T-joints on aluminum alloy plates AA6061-T6, three different levels for each parameter have been selected (rotation speed, transverse speed, type of powder, and groove depth). Other parameters like tilt angle and plunge depth were treated as a constant at 2.5° and 0.3mm respectively. The selected parameters for the FSW process are listed in Table 3.

Taguchi's method is very effective in dealing with multiparameter influenced responses. It is a powerful experimental design tool that dramatically reduces the number of experiments needed to model and optimize the responses [21-23]. The numbers of the parameters of the process taken into account in this study are four and the level of each factor is three. Hence, the four factors with three levels represented the fractional factorial design used is a standard L9 (81) orthogonal array (OA) [24]. This orthogonal array is chosen because of its ability to test the interactions between the variables. Every row of the matrix represents a single trial [25]. Table 4 shows the experimental design based on the OA L9.

3.2. S/N ratio

Taguchi recommends that the ratio of signal to noise (S/N) be used to measure the quality characteristics that deviate from the desired values. There are typically three types of quality characteristics in the study of the S / N ratio, the-lower-better, the-higher-better and the-nominal-better. The S/N ratio for each level of process parameters is computed based on the S/N analysis. Irrespective of the quality attribute group, a higher S/N ratio leads to better quality characteristics [26]. Using a statistical program (MINITABTM® 17), S/N ratio and mean squared deviation (MSD) have been determined by applying Eq. (1 and 2) [27].

$$MSD = \left(\frac{1}{n}\sum_{i=1}^{n}\left(\frac{1}{y_{ij}^2}\right)\right) \qquad (1)$$

$$(S/N)Ratio = -\log_{10}\left(\frac{1}{n}\sum_{i=1}^{n}\left(\frac{1}{y_{ij}^2}\right)\right) \qquad (2)$$

where: y_{ij} = The total trial results , n = Number of trials, i = Trial number, and j = Number of experiment.

3.3. ANOVA examination

The aim of ANOVA is to inspect the significance of the FSW parameters which affect the mechanical strength properties. ANOVA is

utilized to detect the significance of welding parameters statistically. It gives a clear picture of the degree to which the process parameters influence the response and its significance [28].

4. Result and discussion
4.1. Skins ultimate tensile strength

The quality of the welded joints has been described by considering the UTS_{Skins} from hoop test of the stander specimen. The S/N ratio method (larger S/N ratio is better) was adopted to analyze the result and find the optimum level for each welding parameters that maintained the maximum tensile strength in this process. For each experiment, mean tensile strength and S/N ratio are represented in Table 4, while the UTS_{Skins} calculation of the main effect at three different levels (mean and S/N ratio) parameter is shown in Table 5. After checking both tables, and corresponding to a greater mean value and S/N ratio, the computed optimum welding parameters are rotational speed (level 2) =1550 rpm, transverse speed (level 2) =11 mm/min, types of powder (level 1) =Al$_2$O$_3$, and groove's depth (level 2) =1 mm. The variance (Delta) between the greater and the smaller value gives the influence of each factor. So, the most important factors that has influence on UTS_{Skins} for welded parts are groove's depth, rotational speed, types of powder, and transverse speed. The predicted values of the mean are computed using Eq. (3), and the value of UTS_{Skins} from hoop test of the standard specimen exp. 6 can be obtained from stress strain curve as in Fig. 4. The optimum (predicted) values are compared with the obtained values as shown in Table 6.

$$UTS_{Predicted} = \bar{A}_{Nop} + \bar{B}_{Nop} + \bar{C}_{Nop} + \bar{D}_{Nop} - 3\bar{T} \tag{3}$$

where $\bar{T}$ is the total mean tensile strength response, $\bar{A}_{Nop}$; $\bar{B}_{Nop}$; $\bar{C}_{Nop}$; and $\bar{D}_{Nop}$ are the average response at the optimum level of the process parameters.

In order to find the effect of process parameters on various responses, ANOVA technique was performed and the F-values were calculated for various responses to determine the relative significances of different process parameters.

The value of F test gives significant factors that affect the characteristic of the welded parts which were the groove's depth that have the largest value, followed by rotational speed, type of powder, and finally transverse speed as shown in Fig. 5(a).

4.2. Stringers ultimate tensile strength

The second response of the quality of the welded joints has been described by considering the $UTS_{Stringers}$ from T- pull test of the stander specimen. The S/N ratio method was adopted to analyze the result and find the optimum level for each welding parameters that maintained the maximum tensile strength. Table 4 shows the mean tensile strength and S/N ratio, and the $UTS_{Stringers}$ calculation of the main effect at three different levels (mean and S/N ratio) parameter are shown in Table 5. By checking both tables and utilizing the large is better as maximization criteria, the optimum welding parameters are rotational speed (level 1) =960 rpm, transverse speed (level 1) =6 mm/min, types of powder (level 3) =TiO$_2$, and groove's depth (level 2) =1 mm by applying the previous Eq. (3). Fig. 4 gives the obtained values of the $UTS_{Stringers}$ from T-pull test of standard specimen exp. 7. Table 6 gives the mean of the predicted and the obtained values and their conditions.

The value of F test is also used to define which factors of the welding process have an important influence on the characteristic of the welded parts. It appears that the significant factors are the groove's depth that has the largest value, followed by type of powder, rotational speed, and finally the transverse speed as shown in ANOVA chart Fig. 5(b).
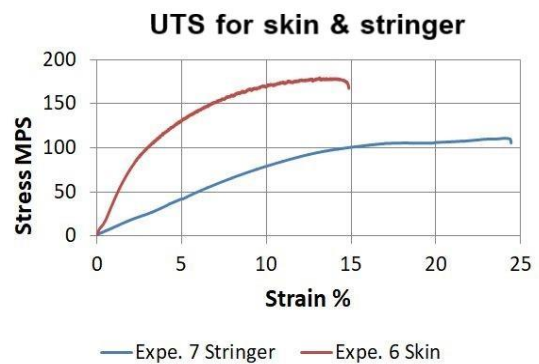
Fig. 4. Ultimate tensile strength for skin and stringer.

Table 4. Experimental design based on the (OA) L9 and experimental results (mean and S/N ratio)   of hoop stress, T-pull stress and HV.

Exp.	A	B	C	D	S/N skin	Mean skin	S/N stringer	Mean stringer	S/N Hardness	Mean Hardness
1	960	6	Al_2O_3	0.5	44.2021	162.5	39.4129	93.5	35.75	61.36
2	960	11	SiC	1	44.2359	163	39.9561	99.5	35.89	62.71
3	960	15	TiO_2	1.5	41.9015	124.5	38.1033	80.5	37.69	77.04
4	1550	6	SiC	1.5	42.0318	126.5	37.1240	72.0	35.33	59.63
5	1550	11	TiO_2	0.5	44.9348	176.5	39.8232	98.0	36.36	66.43
6	1550	15	Al_2O_3	1	44.9578	177	40.2555	103.0	36.83	69.92
7	2000	6	TiO_2	1	43.8838	156.5	40.4771	106.0	35.48	60.03
8	2000	11	Al_2O_3	1.5	42.1684	128.5	35.7560	61.5	35.48	59.52
9	2000	15	SiC	0.5	43.6916	153	37.0226	71.0	36.57	67.81

Table 5. The main effects of UTSskin, UTSstringer, and HV.

	S/N ratio for skin response				S/N ratio for stringer response				S/N ratio for hardness			
Levels	A	B	C	D	A	B	C	D	A	B	C	D
1	43.45	43.37	43.78	44.28	39.16	39.00	38.47	38.75	36.45	35.53	36.03	36.23
2	43.97	43.78	43.32	44.36	39.07	38.51	38.03	40.23	36.18	35.91	35.93	36.07
3	43.25	43.52	43.57	42.03	37.75	38.46	39.47	36.99	35.85	37.04	36.52	36.17
Delta	0.73	0.41	0.46	2.33	1.41	0.54	1.43	3.24	0.60	1.51	0.58	0.16
Rank	2	4	3	1	3	4	2	1	2	1	3	4

	Means for skin response				Means for stringer response				Means for hardness			
Levels	A	B	C	D	A	B	C	D	A	B	C	D
1	150.0	148.5	156.0	164.0	91.17	90.50	86.00	87.50	67.04	60.34	63.60	65.20
2	160.0	156.0	147.5	165.5	90.00	86.33	80.83	102.83	65.33	62.89	63.39	64.22
3	146.0	151.5	152.5	126.5	79.50	84.83	94.83	71.33	62.46	71.59	67.84	65.46
Delta	14	7.5	8.5	39.0	11.67	5.67	14.00	31.50	4.59	11.25	4.45	1.18
Rank	2	4	3	1	3	4	2	1	2	1	3	4

Table 6. Optimum (predicted) and obtained values for quality characteristics.

Quality	Predicted condition	Predicted value	Obtained condition	Obtained value
UTS$_{skin}$	A2, B2,C1, D2 1550 rpm,11m/min, Al_2O_3, and 1 mm.	181.5 MPa	A2, B3,C1, D2 1550 rpm, 15 mm/min, Al_2O_3, and 1 mm.	177 MPa
UTS$_{stringer}$	A1, B1, C3,D2 960 rpm, 6 mm/min, TiO_2, and 1 mm.	117.667 MPa	A3, B1, C3,D2 2000 rpm, 6 mm/min, TiO_2, and 1 mm.	106 MPa
HV	A1, B3, C3, D3 960 rpm, 15 mm/min, TiO_2, and 1.5 mm	77 HV	A1, B3, C3, D3 960 rpm, 15 mm/min, TiO_2, and 1.5 mm	77 HV

4.3. Hardness

Fig. 6 shows the hardness profile along skins and stringers plate. With regard to the stringer the hardness is taken from the top of the skin plate to the end of the stringers. The shape of the profile appeared as "N" shape shown in Fig. 6(a), due to uneven distribution of the welding temperature through skin thickness. The maximum value of the hardness in welding zone has appeared far away 1.5 mm from the top surface, where the agglomeration and distribution of nano-powders concentrate in this region. While "W" shape of the hardness profile along the skin plate appeared as shown in Fig. 6(b), it can be seen that the hardness reaches its higher value at point of a 1.75 mm from the center of the nugget zone (NZ) experiment No. 3, farther from this point the hardness decreases till it reaches the minimum value at the thermo mechanically affected zone (TMAZ) and then increases again up at the unaffected zone reign. This indicates that the hardness enhanced inside the composite zone and softened around this area. The increases in hardness were not significantly high, because improper dispersion of nanoparticles in the matrix is related to the one pass of FSW.

The same technique (S/N) ratio method was used to analyze the results and obtain the optimal level for each process parameter to ensure the maximum value of microhardness during the FSW process. The microhardness results (mean), and (S/N) ratio are given in Table 4, and the microhardness calculation of the main effect at three different levels (mean and S/N ratio) parameter are shown in Table 5. Based on that, the optimum condition of the main at [rotational speed (level 1) =960 rpm, transverse speed (level 3) =15 mm/min, types of powder (level 3) =TiO$_2$, and groove's depth (level 3) =1.5 mm] is given. Table 6 gives the mean of the predicted and obtained values and their conditions.

From ANOVA hardness chart Fig. 5(c), the significant factors that affected the quality characteristic of the welded parts are transverse speed which has the largest value, followed by the types of powder, rotational speed, and finally the groove's depth.

(a)

(b)

(c)
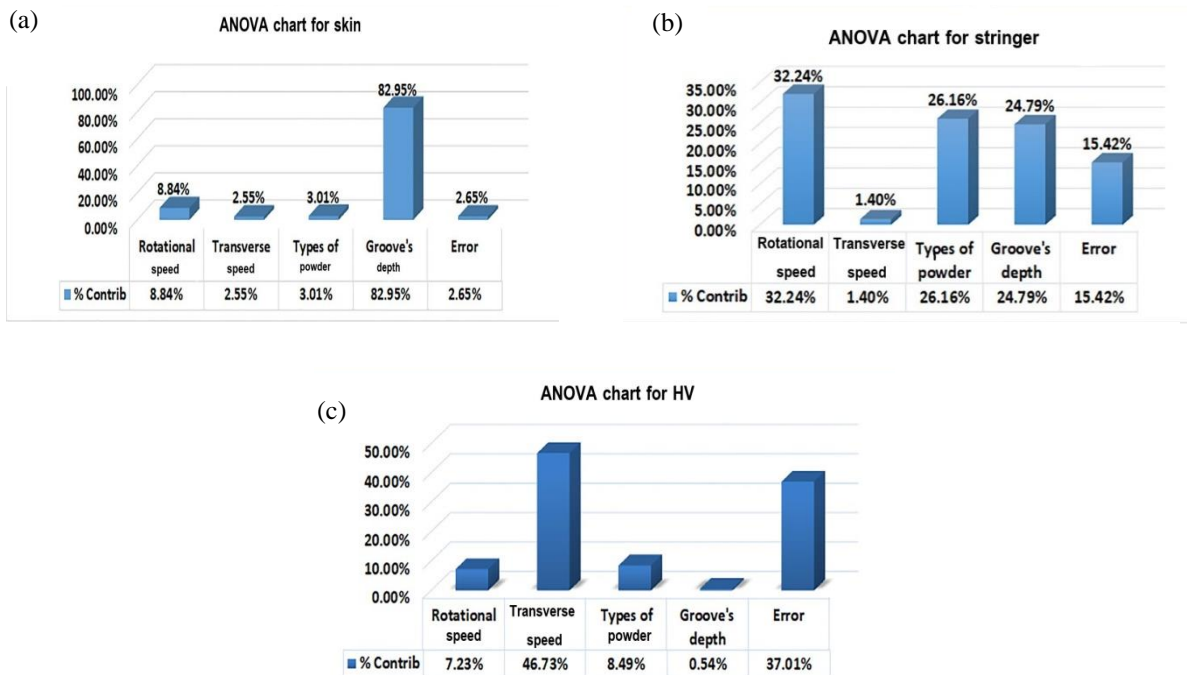
Fig. 5. Contribution effect of process parameters; (a) skin, (b) stringer, and (c) micro-hardness.
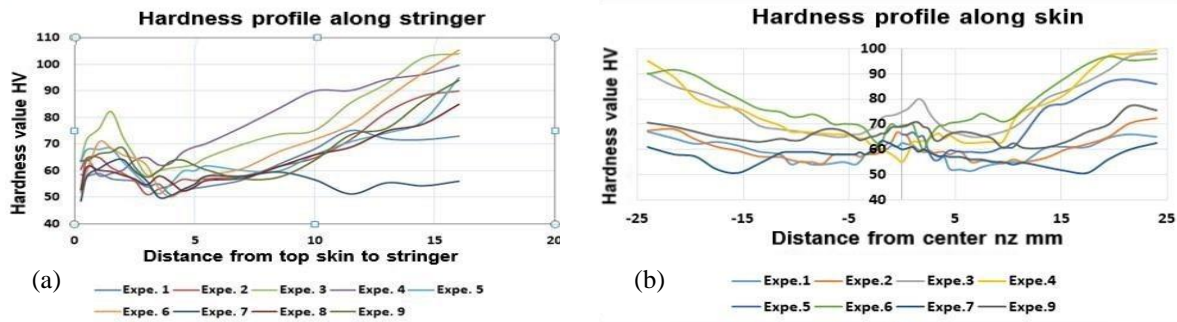
Fig. 6. Vickers hardness profile along; (a) stringers plate and (b) skins plate.
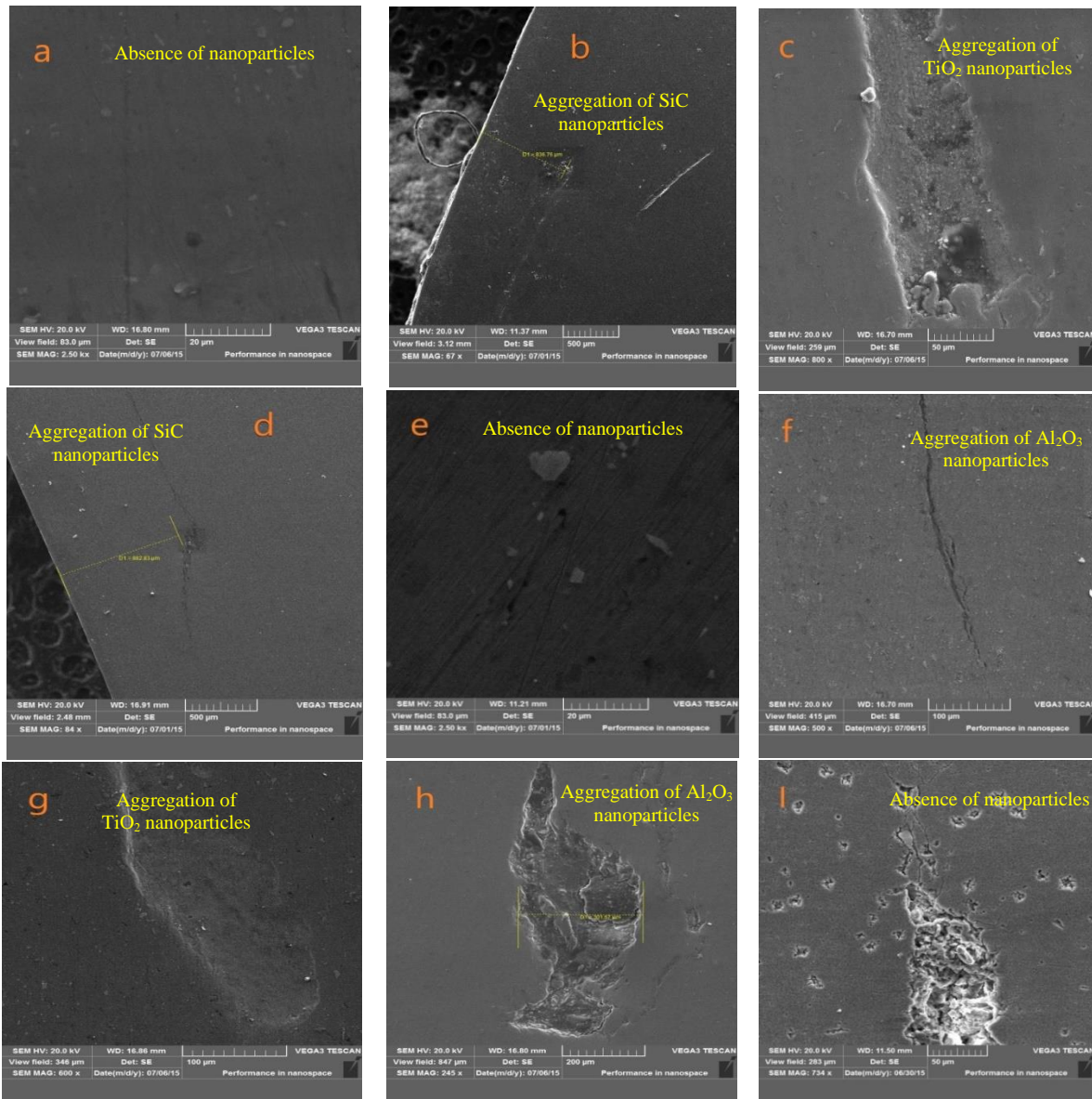
Fig. 7. SEM images for all experiments; (a) exp.1, (b) exp.2, (c) exp.3, (d) exp.4, (e) exp.5, (f) exp.6, (g) exp.7, (h) exp.8, and (I) exp.9.
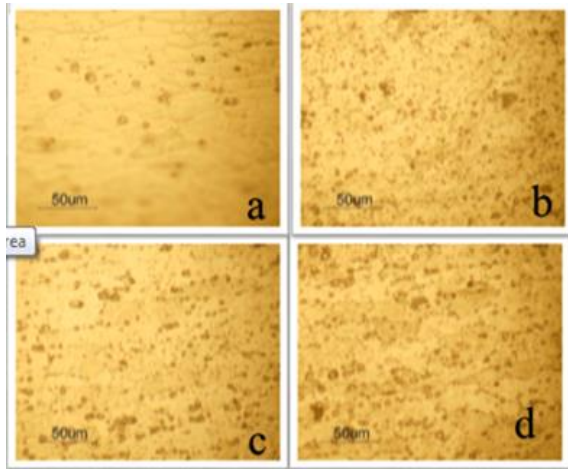
Fig. 8. Optical micrographs; (a) base metal, (b) nugget zone, (c) thermo mechanically affected zone, and (d) heat affected zone.

4.4. Microstructure

The aim of this examination is to identify the distribution of nano-powders in nugget zone and the amount embedded in the matrix, and understand the effect of process parameters on the operation of making the MMNCs. After one pass of FSW with different relative contents of nano-powders, the SEM micrograph appearance of nuggets zone for the nine experiments are shown in Fig. 7. The aggregation of nano-powders could be observed in the MMNCs and the nanoparticle distribution in all the samples fabricated by these process parameters is irregular due to the one pass of the FSW. A similar effect of more than one pass on the cluster particles in the MMNCs has been reported by other researchers [29-31] in which the distribution of nanoparticles was found to be uniform related to more one pass of FSW.

According to the result obtained from the UTS_{skin}, Exp. (6) was selected as the best result among the obtained experiments. Fig. 8 shows the optical micrographs of the surface hybrid composites in three zones and its base metal. It is obvious that the grain size distributions within the nugget zone has quite fine grains in comparison to other regions. The grains in the stir zone (SZ) experienced severe plastic deformation and recrystallization. Six random samples were chosen to measure their affected area, the average area of the base metal and

nugget zone are 31116.97 μm^2, and 17406.97 μm^2 respectively.

5. Conclusions

In this work, the T- joints were fabricated and investigated at different welding conditions and the influences of reinforcement nano-powders Al_2O_3, SiC and TiO_2 on the mechanical properties of Al alloy 6061-T6 were studied. The following conclusions are obtained,

- The additions of nano-powders particles in the region of FSW improve the ultimate tensile strength and hardness, but the agglomerations of the powder in this region will reduce the improvement of these properties.
- Tensile properties in optimal shape (i.e. at predicted condition A2, B2, C1, D2 for skin and A1, B1, C3, D2 for stringer) are less than the base material due to the presence of reinforcement particles which make the matrix more brittle.
- Hardness value in the nugget zone is higher than other regions, but remained less than the base metal, due to the cluster and non-uniform distribution of the nano-powders in welding region.
- The dispersion of nano-powder particles in Al matrix cannot be uniformly distributed by the use of one pass of FSW.

References

[1] No. 5, 460, 317. U. S. Patent "*Friction Stir Butt Welding*" W. Thomas, E. Nicholas, J. Needham, M. Murch, P. Smith, and C. Dawes, (1995).

[2] H. Bakes, D. Benjamin, C. W. Kirkpatrick. *Metal's Handbook*, Vol. 2. ASM, Materials Park: OH, pp. 3–23, (1991).

[3] N. Ravi, D. Sastikumar, N. Subramanian, A. Nath and V. Masilamani, "Microhardness and microstructure studies on laser surface alloyed aluminum alloy with Ni-Cr", *J. Mater. Manuf. Proc.*, Vol. 15, No. 3, pp. 395-404, (2000).

[4] S. Amin, M. Hanna and A. Mohamed, "Experimental Study the Effect of Tool Design on the Mechanical Properties of Bobbin Friction Stir Welded 6061-T6 Aluminum Alloy", *AL-Khwarizmi Eng. J.*, Vol. 14, No. 3, pp. 1- 11, (2018).

[5]   T. Clyne and P. Withers, *An introduction to metal matrix composites*. Cambridge [England]: New York : Cambridge University Press, (1995).

[6]   G. Kiourtsidis and S. Skolianos, "Wear behavior of artificially aged AA2024/40 μm SiCp composites in comparison with conventionally wear resistant ferrous materials", *Wear*, Vol. 253, No. 9-10, pp. 946-956, (2002).

[7]   B. Zahmatkesh and M. Enayati, "A novel approach for development of surface nanocomposite by friction stir processing", *Mater. Sci. Eng. J. A*, Vol. 527, No. 24-25, pp. 6734-6740, (2010).

[8]   F. Khodabakhshi, A. Gerlich, P. Svec, "Fabrication of a high strength ultra-fine grained Al-Mg-SiC nanocomposite by multi-step friction-stir processing", *Mater. Sci. J.: A,* Vol. 698, pp. 313-325, (2017).

[9]   E. Rabinowicz, *Friction and wear of materials*. New York: JohnWiley and Sons, (1995).

[10] K. G. Budinski. *Surface engineering for wear resistance*. New Jersey: Prentice-Hall; (1988).

[11] G. Zhou, X. Yang, L. Cui, Z. Zhang and X. Xu, "Study on the microstructures and tensile behaviors of friction stir welded T-joints for AA6061-T4 alloys", *J. Mater. Eng. Perfo.*, Vol. 21, No. 10, pp. 2131-2139, (2012).

[12] F. Mustafa, A. Kadhym and H. Yahya, "Tool geometries optimization for friction stir welding of AA6061-T6 aluminum alloy T-joint using Taguchi method to improve the mechanical behavior", *J. Manuf. Sci. Eng.*, Vol. 137, No. 3, pp. 031018-8 pages, (2015).

[13] S. Tavares, P. Azevedo, B. Emi´lio, V. Richter, M. Figueiredo, P. Vilac¸a, P. de Castro "Friction stir welding of T-joints in dissimilar aluminum alloys." *ASME Int. Mech. Eng. Cong. Expos.*, Vol. 4, No. 67522, pp. 265-273, (2008).

[14] D. Lim, T. Shibayanagi and A. Gerlich, "Synthesis of multi-walled CNT reinforced aluminium alloy composite via friction stir processing", *Mater. Sci. Eng.*

[15] A. Shafiei, S. Kashani, and A. Zarei, "Microstructures and mechanical properties of Al/Al$_2$O$_3$ surface nano-composite layer produced by friction stir processing", *Mater. Sci. Eng. J. A*, Vol. 500, No. 1-2, pp. 84-91, (2009).

[16] M. Azizieh, A. Kokabi and P. Abachi, "Effect of rotational speed and probe profile on microstructure and hardness of AZ31/Al$_2$O$_3$ nanocomposites fabricated by friction stir processing", *Mater. Des. J.* Vol. 32, No. 4, pp. 2034-2041, (2011).

[17] E. Mahmoud, M. Takahashi, T. Shibayanagi and K. Ikeuchi, "Wear characteristics of surface-hybrid-MMCs layer fabricated on aluminum plate by friction stir processing", *Wear*, Vol. 268, No. 9-10, pp. 1111-1121, (2010).

[18] M. Salehi, M. Saadatmand and J. Mohandesi, "Optimization of process parameters for producing AA6061/SiC nanocomposites by friction stir processing", *Trans. Nonfer. Met. Soc. China*, Vol. 22, No. 5, pp. 1055-1063, (2012).

[19] Z. Du, M. Tan, J. Guo, J. Wei, "Friction stir processing of Al–CNT composites", *Proc. of the Inst. of Mech. Eng., Part L: J. Mater. Des. Appl.*, Vol. 230, No. 3, pp. 825-833, (2016).

[20] A. Takhakh, H. Abdulla, "Surface modification of AA 7075-T651 plate using friction stir processing with SIC particles", *Emirates J. Eng. Res.*, Vol. 22, No. 3, pp.1-11, (2017)

[21] A. Devaraju, A. Kumar, A. Kumaraswamy and B. Kotiveerachari, "Influence of reinforcements (SiC and Al$_2$O$_3$) and rotational speed on wear and mechanical properties of aluminum alloy 6061-T6 based surface hybrid composites produced via friction stir processing", *Mater. Des. J.*, Vol. 51, pp. 331-341, (2013).

[22] F. Alkaabneh, M. Barghash and Y. Abdullat, "A Novel Statistical Analysis for Residual Stress in Injection Molding",

American J. Oper. Res., Vol. 6, No. 1, pp. 90-103, (2016).

[23] S. Juang and Y. Tarng, "Process parameter selection for optimizing the weld pool geometry in the tungsten inert gas welding of stainless steel", *J. Mater. Proc. Tech.* Vol. 122, No. 1, pp. 33-37, (2002).

[24] Sung. H. "*Robust Design and Analysis for Quality Engineering*", Park Chapman and Hall, London, (1996).

[25] J. Ghani, I. Choudhury and H. Hassan, "Application of Taguchi method in the optimization of end milling parameters", *J. Mater. Proc. Tech.*, Vol. 145, No. 1, pp. 84-92, (2004).

[26] W. Yang and Y. Tarng, "Design optimization of cutting parameters for turning operations based on the Taguchi method", *J. Mater. Proc. Tech.* Vol. 84, No. 1-3, pp. 122-129, (1998).

[27] Minitab Company, "MINITABTM Statistical Software Release 16," Minitab Inc., State College, PA, http://www.minitab.com

[28] M. Shojaeefard, A. Khalkhali, M. Akbari and M. Tahani, "Application of Taguchi optimization technique in determining aluminum to brass friction stir welding parameters", *Mater. Des.*, Vol. 52, pp. 587-592, (2013).

[29] J. Guo, J. Liu, C. Sun, S. Maleksaeedi, G. Bi, M. Tan and J. Wei, "Effects of nano-Al_2O_3 particle addition on grain structure evolution and mechanical behaviour of friction-stir-processed Al", *Mater. Sci. Eng. J. A*, Vol. 602, pp. 143-149, (2014).

[30] A. Shahi, M. Sohi, D. Ahmadkhaniha and M. Ghambari, "In situ formation of Al–Al3Ni composites on commercially pure aluminium by friction stir processing", *Int. J. Adv. Manuf. Tech.*, Vol. 75, No. 9-12, pp. 1331-1337, (2014).

[31] C. Lee, J. Huang and P. Hsieh, "Mg based nano-composites fabricated by friction stir processing", *Scripta Mater. J.*, Vol. 54, No. 7, pp. 1415-1420, (2006).

How to cite this paper: